INTRINSIC FEEDBACK FACTORS PRODUCING INERTIAL COMPENSATION IN MUSCLE

LLOYD D. PARTRIDGE

From the Department of Physiology and Biophysics, University of Tennessee, Memphis, Tennessee 38103

ABSTRACT An attempt was made to determine the factors causing the load-inertia compensation that has been observed in skeletal muscle. Cat skeletal muscle force output was determined as a function of the two variables, length and stimulus pulse rate. The results were represented in a system diagram from which it becomes apparent that: (*a*) the length-tension relationship in muscle forms a functional, nonneural servo feedback; (*b*) the force-velocity curve appears as an oscillation-damping, velocity feedback in the muscle servo; (*c*) the nonlinear action of pulse rate on response is, in effect, in the input element to the muscle servo system. For purpose of analysis of the motor system it appears that these signal handling characteristics of muscle make it more nearly a "position servo" than a "force motor."

In the control of movement the need for adjustment of forces to compensate for inertial effects is a well known problem (4, 5). In a little known paper, it was first proposed that the stretch reflex was a feedback system with anterior horn cell input (20) which could account for inertial compensation. However, it was not until after the recognition of the role of the γ fibers (11) and the general development of feedback theory, that the servo type action became commonly ascribed to this reflex (12). More recently it has been demonstrated that muscle alone without reflex feed back can show an appreciable inertial compensation effect (15).

Inertial compensation in this muscle was demonstrated by three different criteria. The load-moving muscle was subjected to sinusoidally modulated stimulus pulse rates while the phase and amplitude relationships between stimulus cycle and movement cycle were measured. Over most of the physiological range the theoretical 180° phase lag of the inertial load was almost completely compensated. Also in amplitude vs. load graphs and amplitude vs. frequency graphs an almost complete compensation for inertia was shown. Thus the response to a particular input stimulus rate modulation had a near constant amplitude in spite of a 28 to 1 variation of load inertia. Similarly, with a constant rate modulation amplitude the response was independent of stimulus cyclic frequency over most of the physiological range.

From basic Newtonian considerations, it is obvious that for the movement amplitude to remain constant, the force amplitude at the test frequency must have increased in proportion to the load inertia. The force amplitude must also have changed with the square of the frequency. The implications of this basic mechanical relationship, when applied to the experimental results, is the rather dramatic conclusion that the force delivered by the muscle to the load, at the signal frequency, must have varied by almost 10,000 times depending on the load impedance (Fig. 1). This figure represents the calculated approximate force amplitude at each frequency for a series of different test frequencies and load inertias based on the amplitude data from the muscle load moving study (reference 15, Fig. 4). When these results are presented in this form the magnitude of the force compensation is easily seen. It is

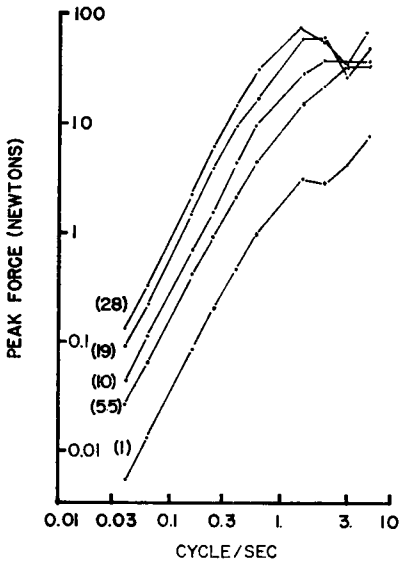

FIGURE 1 Review of effect of load inertia and signal frequency on force delivered by muscle to loads. All stimulations were cyclically modulated pulse rates, changing from 5 to 35 pps at the frequencies indicated on abcissa. Numbers in parentheses represent relative moment of inertia of load for each curve. Points were calculated from amplitude data used in a previous study (reference 15, Fig. 4). All points on this graph are from one circulated muscle under stable response conditions and are typical of whole test series. Since pulse rate-signal amplitude was constant (5–35 pps), force variation seems to be entirely due to inertia and frequency-dependent load impedance.

also of interest to note that in the high-frequency high-load range where compensation failed the forces involved are in the maximum range developed by this muscle. Although such calculations are subject to several errors it is clear that the inertial compensation factor does represent so large a force adjustment that it must be considered in the analysis of motor control.

In that experiment the nerve stimulus was independent of the load position so the compensation must have occurred within the muscle itself. The force was determined by the stimulus and also by a function of the load. It was argued that this effect could be represented as a functional feedback in which stimulus pattern and load position interacted to determine the force delivered to the load. The present study identifies a probable mechanism of that feedback compensation. The characteristics of the feedback were sought by measurement of the length, pulse rate, and force relationship in loaded muscle.

METHOD

In order to measure length, nerve impulse rate, and force interrelationships several approaches are possible. In the present studies, stimulus pulse rate was slowly increased while force was maintained constant and muscle length measured. Since over-all movement was slow and in air, both inertial reactive force and viscous forces were near zero. For these conditions constant force was produced by use of a set of fixed gravity loads.

Supramaximal stimulus pulses were delivered to the cut motor nerves supplying circulated triceps sura muscles of nembutal-anesthetized cats. The cut tendons were wired to a differential transformer position transducer and a simple weight load. The femur and tibia were rigidly clamped. The muscle temperature was maintained near constant at 36°C using thermistor-controlled radiant heat. Repeated tests showed the system response to be stable. Stimulus rate was increased from essentially 0–40 pulses/sec (pps) at a rate of 1 pulse/sec^2. Pulse rate vs. position was recorded directly on an X-Y plotter. Muscle length and limb mechanics measurements were made to allow comparison of the test lengths with physiological positions. All observed response patterns were similar although quantitative differences were seen between different cats in a direction roughly related to cat size. In this series, load weights (including transducers) ranged from 500 to 3,000 or 4,000 g in 500 g steps.

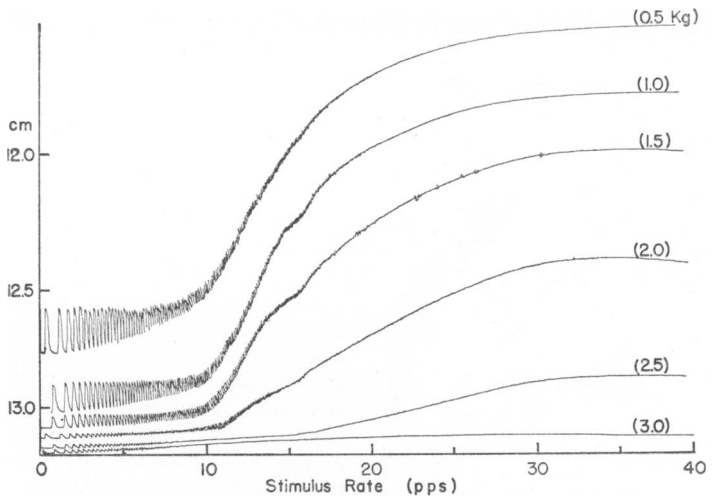

FIGURE 2 Effect of load and stimulus pulse rate on muscle length. Parenthetic numbers show weight attached to muscle for each recorded line. Pulse rate increased from near 0 to 40 pps at 1 pps^2. Length scale is based on measurement of distance from gastrocnemius origin to insertion and includes tendon length, thus recorded length differences are much more precise than absolute length.

To display better the length-force trade-off effect, the directly recorded family of length vs. pulse rate curves were measured and regraphed in the length vs. tension plane as a family of different pulse rate lines representing 5 pps intervals from 0 to 40 pps.

RESULTS

Fig. 2 shows the length vs. pulse rate relationship for one muscle. The sigmoid shape of this curve does not greatly differ from that of graphs drawn in student

laboratory experiments relating sampled isotonic contraction height data to stimulus rate from experiments with static tetanic train stimulus. Thus: (*a*) at low rates nonfused single twitches are demonstrated; (*b*) most of the stimulus pulse rate effect on length occurs over a relatively restricted range, in this muscle between 10 and 20 pulses/sec; (*c*) at high stimulus rates the fused contracted length shows little further stimulus rate dependence. (Because in the present study the load inertias were high, the individual twitches fused at much lower rates than would be expected in conventional low inertia isometric or isotonic recording, and the tetanus to twitch height ratio was large.)

Each load increase resulted in a definite offset of the position–pulse rate curve, up to the point that the load was so great that near isometric responses occurred.

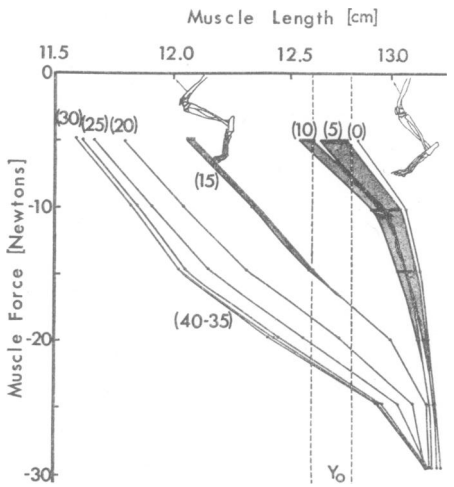

FIGURE 3 Effect of length on muscle force, at different stimulus pulse rates. Stimulus pulse rate, in pulses/second, for each line is shown in parentheses. An approximate equivalent skeletal position for two different lengths is sketched. Amplitudes of nonfused contraction movements are represented by stippled areas.

The resulting family of curves for different loads in effect makes this figure a three dimensional graph relating pulse rate, force, and length. The different pulse rate–length curves are similar over a considerable range of loads. However, with increasing loads the slope of the curves changed, reaching near zero with the largest loads. It is also clear from this graph that for any given pulse rate, length is markedly dependent on load as well as on pulse rate but by replotting the data into the length vs. force plane, this relationship is more easily seen.

Fig. 3 shows the effect of length on force delivered by that muscle for each of a series of nine different stimulus rates. For these graphs muscle force was assumed to be identical in size to gravity force (maximum acceleration correction of the smoothed graph never exceeds 0.002 newtons). This muscle force-length graph is plotted in the fourth quadrant because muscle force is measured in a direction opposite to muscle length. (The usual length-tension diagram, where sign is unimportant, is plotted in the first quadrant.) The length vs. force lines based on 35–40 pps stimula-

tion are in fact that part of the conventional tetanic length-tension graph representing lengths, Y, equal to and shorter than resting body length, Y_0. The remaining length-tension lines of this figure represent lower stimulus rates and include nonfused contraction and even the nonstimulated muscle length–tension curve. For this muscle at lengths greater than about 12.8 cm the slope $\frac{\partial F_M}{\partial Y}$, of all of the lines is considerably steeper than at shorter lengths. This greater stiffness of the stretched muscle probably involves connective tissue stretching. Rest body length of the muscle is 12.6 cm if based on the point at which tension first deviates from zero or 12.8 cm if based on the best approximation we were able to make to relaxed muscle length in situ.

For purpose of later analysis this graphically illustrated relationship can also be stated as empirical equations. The active muscle force at resting length, F_0, is a nonlinear function of the stimulus pulse rate, R, i.e.,

$$F_0 = f(R) \tag{1}$$

(In nonfused contractions F_0 would represent the effective mean force.) The relationship, shown on the graph, between length and the corresponding muscle output force, F_M, for a particular pulse rate is described as:

$$F_M = F_0 + \int_{Y_0}^{Y} \frac{\partial F_M}{\partial Y}\, dY \tag{2}$$

For any region including Y_0 in which the slope is a constant, K, equation 2 would reduce to:

$$F_M = f(R) + K(Y - Y_0) \tag{3}$$

For the particular muscle represented by Figs. 2 and 3 a slope, $K \approx -1740$ newtons/meter, approximately represents the curves in the region $Y < Y_0$. For lengths greater than Y_0 the slope of the total length tension curve markedly increases but shows no sign change. In the region to the left of Y_0 the length-tension relationship for tetanic stimulus for whole muscle is comparable to that determined for the single sarcomere (7), so the same approximate description could be applied to the single sarcomere as well as to the gross muscle.

Length-tension relationships have been derived with a variety of different techniques, all of which seem to influence details of the response. The standard tests, run in student laboratory with tetanic stimulus and preset lengths, give results similar to those described above. The responses illustrated, Figs. 2 and 3 represent the product of the procedure which gave the most reproducible results in our hands. This procedure involved the removal of load for a 1–2 min period of rest between stimulus trains. In this rest period a single stimulus was given to restore the rest length. When this procedure was applied to a cat in good condition, the first and last

test in a series could often be superimposed with no deviations larger than the recording noise. Quantitative differences between different cats were sometimes large but the qualitative form of the graph was quite similar from one cat to another, as long as the circulatory function was stable. Tests run without unloaded rest periods showed a slow plastic stretching of the muscle. In such experiments, if the early records (where stretching was fast) are eliminated, the remaining results are essentially the same as those in experiments done with more careful control.

Additional experiments using quite different test details were also explored. Preliminary tests were directly recorded in the length-tension (work) plane. For these tests the muscle was stretched during a steady stimulus period. The results were similar to Fig. 3 but much less repeatable. Other tests in the stimulus rate–tension (isometric) plane were run, producing a few families of curves for different lengths. When these data are remapped into the work plane the results are comparable to those obtained in Fig. 3 from the load-moving test. As has been described previously, the use of decreasing pulse rate sequence produces quantitatively different results than increasing pulse rate tests (15). This direction of change of stimulus rate effect was seen in both isometric and load-moving tests. In spite of these variations of details, it appears that the general pattern described for the length-tension trade off is characteristic of muscle through a wide variety of conditions of operation.

DISCUSSION

In a study of muscle's movement of load in response to dynamic pulse rate–stimulus patterns (15) the input-output characteristics were described. This description was first without reference to the internal interrelationships between the components within the test system, that is, the system was looked upon as a single block, Fig. 4 *a*. This block had a pulse rate input and load-position output. Such a view is useful when it is only desired to consider how this muscle-load block would behave in a larger system, e.g., a reflex. There it is possible to use data so acquired without consideration of the factors involved within the block. However, when the characteristics of the inertial components within the block are considered, it becomes apparent that, as reviewed in Fig. 1, the inertial impedance of the load greatly modifies the load moving force delivered by the muscle.

To explain this observed force adjustment, in tests without a functioning neural feedback, it was necessary to presume a feedback effect within the muscle itself (15). Fig. 4 *b* schematically represents this functional feedback. This diagram shows the force, F_M, delivered by the muscle to its load, as a function of two variables, length and pulse rate. The present study provides the graphic representation (Fig. 3) of the length, pulse rate, and force relationship of the feedback within the muscle block. It can be seen that for a particular pulse rate there would be one equilibrium length at which the force delivered by the muscle would just balance the load on that muscle. The inertial impedance of the load would not have any effect on this static null posi-

tion. Furthermore the null position is a nonlinear function of pulse rate. A deviation from the pulse rate–determined null position would cause a force change in a direction which would tend to return the load to this null position. Stimulus pulse rate determines null position and thus, on a static basis, it would appear that length-

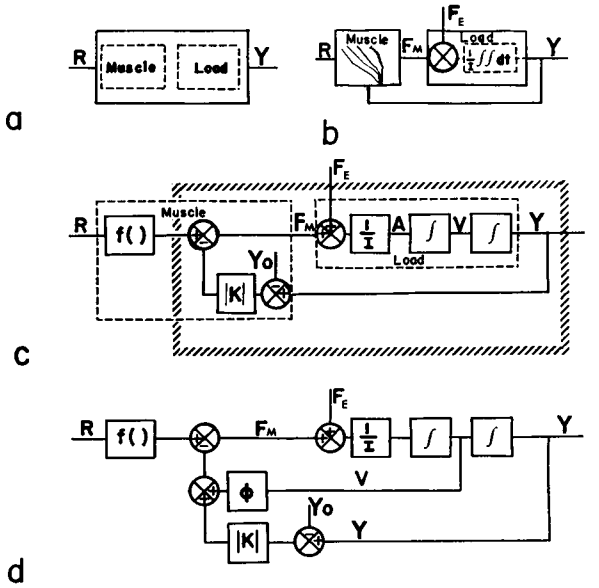

FIGURE 4 Progressive development of functional block diagram of loaded muscle. (*a*) Single block representation, adequate for frequency response study of movement amplitude. R = input, pulse rate; Y = output, position. (*b*) Expanded block diagram of loaded muscle with externally applied force, F_E, and muscle force, F_M, considered. Feedback is added between load position and muscle, representing F_M dependence on response. The length-rate-force graph (Fig. 3) is inserted as muscle characteristics relating R and Y to F_M. I = load moment of inertia. (By measuring both muscle length and load position as distance between gastrocnemius origin and point of tendon attachment on load the value $Y \equiv$ muscle length $\equiv$ load position.) (*c*) Block diagram equivalent of *b* for the physiological muscle length range in which length-tension slope, K, is essentially constant. $f(\ )$ = nonlinear effect of stimulus pulse rate on muscle response. Broken lines enclose blocks representing muscle and load. Hatched line enclosed functional feedback system, produced by action of length-tension effect. Symbols in each block represent action of block. Y_0 = resting muscle length, A = acceleration, V = velocity. (*d*) Servo system type diagram, equivalent of loaded muscle system, with impulse rate input (R), position output (Y), length-tension feedback with coefficient K, nonlinear dependence on stimulus rate signal, $f(\ )$, and nonlinear force-velocity feedback coefficient, ϕ.

tension feedback would accomplish the necessary corrections. Of course, as is characteristic of such simple feedback systems, for any load there should be a residual error.

The dynamics of the system also must be considered. The dynamic characteristics of the load are described by the laws of Newtonian mechanics. The summed forces

divided by an inertial constant, I, determines the acceleration of the test load. (In the experiments in question no spring, viscous, or frictional effects of measurable size existed, and load geometry was simple, thus the necessary calculation is minimal.) The usual (two) time integrations between acceleration and position are taken with an initial condition of zero velocity. To examine the system dynamics the block diagram is again expanded to a more detailed equivalent, Fig. 4 *c*. The block diagram of load in Fig. 4 *c* is an exact equivalent of the equations of Newtonian mechanics and is thus a very close analogue of the load used in the experiments. The block diagram representation of muscle is similar to equation 3, thus approximating the pulse rate–length–force relationship measured in muscle over much of the operating range. In Fig. 4 *c* these two blocks are interconnected, as required by the physical system which can be seen to be the diagram of a typical negative feedback system. For this system some lag and the nonlinearities appear in the input element. [It might be noted that the input block characteristics are equivalent to isometric muscle response characteristics (14). That is a test condition in which Y is constant and $F_B = -F_M$.] The linear closed loop system within the hatched line is easily analyzed by standard methods. The loop gain would be load and frequency dependent, changing inversely with load inertia and inversely with the square of frequency. For the muscle represented in Figs. 2 and 3, loaded with 1 kg, the loop gain would be 1 at about 6.6 cycles/sec while at 0.66 cycles/sec the gain would be 100. If the load inertia was only the size represented by the foot moving around the ankle, the gain would be 30–50 times larger at each frequency. From standard feedback system calculation (19) these loop gain values are clearly large enough to account for the several thousandfold force adjustment which appears in the previously observed load-moving response curve (Fig. 1). It would also be predicted that this inertial compensation might begin to fail with large loads at high frequency. Although the point where this failure should become apparent is near the upper frequency and load range that has been tested, this effect does appear to occur (reference 15, Figs. 4, 6, 10).

These linear feedback calculations with appropriate bias values can be applied in any region where the length-tension graph is linear. For much of the physiological range this approximation is reasonable. However, in the range of muscle lengths greater than Y_0, an abrupt increase of slope is encountered. Also since muscle produces no negative forces, slope approaches zero at very short lengths. For this particular muscle it is our impression that these very nonlinear regions are seldom reached in normal operation. If these regions are considered, the nonlinearities appreciably complicate analysis, but since no sign change is found in the slope of the graph the effect of the nonlinearities on equilibrium position is only quantitative. For a small amplitude length change, even in these regions, the graph would appear near linear and the system could be treated as linear using a different value for K and Y_0. Where the stiffness is mainly contributed by connective tissue, the positioning effect is mainly passive but would appear like a control system of increased gain. If the muscle ever becomes slack, in physiological operation, its effective feedback gain

would be zero and all positioning effects would depend only on the antagonist's action, presumably acting in its stiff range. It is quite possible that antagonist pairs are so set in length that these nonlinearities are almost entirely canceled in their joint action, but the several variables involved are not well enough known to calculate how good this linearization is.

The dynamic phase-shifting effect must also be considered. By conventional block diagram algebra (19) it can be shown that a block diagram functionally equivalent to Fig. 4 *c* exists in which the two summing points for Y_0 and F_E are transferred outside the loop. When this is done the loop remaining in the equivalent diagram is a phase shift oscillator with a natural frequency, $f_n = \frac{1}{2\pi}\sqrt{\frac{K}{I}}$. For the muscle represented in Fig. 3 with a 1 kg load, $f_n = 6.6$ Hz. An oscillation of this frequency could have been recorded readily by the instruments used in the experiment and was not (Fig. 2). In fact, even when sharp transients were introduced, in the form of single widely spaced stimulus pulses, no appreciable free oscillation was produced. Furthermore, except in some insect muscles (16) a loaded muscle does not generally behave, like a loaded spring, as an oscillator, although it does show well damped oscillation.

Since these predictions do not match observations the model is inadequate However, the model is entirely based on known parts and experimentally determined characteristics. It therefore appears that the model is incomplete rather than wrong. The difference between the real system and the model is in the fact that the real system shows considerable damping but the model does not. In a system of this type, damping can be accomplished by a velocity feedback such as is added in Fig. 4 *d* with a coefficient of ϕ. If this type of feedback exists in muscle it could account for the observed damping. Examining the force-velocity experiments of Fenn and Marsh (6), Hill (8), and Aubert (2), it is seen that their results do show a velocity-dependent decrease of the force applied to the load. For each of their experimental force-velocity relationships to fit into Fig. 4 *d*, the damping feedback coefficient ϕ must be considered to be a positive variable. Such a nonconstant damping coefficient complicates detailed prediction of the exact performance of the system. However, even though nonlinear, this system description and diagram does show the functional relationship between the three separately known functions: pulse rate vs. tension; length vs. tension; and force vs. velocity.

Some of these relationships have previously been combined for analysis. Although in the original studies of force-velocity relationships only a shortening muscle and a constant, F_0, were tested, Abbott and Wilkie (1) later showed that the force-velocity relationship could be extrapolated to apply at different lengths if the length-tension effect on F_0 was taken into consideration. Still later Jewell and Wilkie (10) showed that, in the relaxing muscle with a time-changing F_0, it is still possible to make fair approximations of observed results with the same force-velocity equations. It now appears that the length vs. tension effect should be combined

with the impulse rate vs. tension relationship, to account for the several thousand-fold force adjustment observed as an inertial compensation, in muscle, following a changing pulse rate command to move a load. Whether Fenn and Marsh's (6), or Hill's (8), or Aubert's (2) empirical description of the force-velocity curve is used, the force-velocity relationship described would have a damping action. In each case the damping coefficient, ϕ, would change nonlinearly as a function of both V and F_0. Thus, the force-velocity effect would provide all or part of the necessary damping for the length-tension feedback system. Since force-velocity and length-tension effects, and changing F_0 do interact in other cases, it is not surprising that they should interact when F_0 changes with motor nerve impulse rate.

Even though these previous studies of the length-tension and force-velocity effects were not expressed in feedback terms, it can be shown that the calculations are equivalent to feedback calculations. These calculations, however, did omit the concept of an input, which is necessary to make signal-following consideration possible. A signal-following feedback diagram representation has also been used for force-velocity effect (9) and the length-tension effect (13). Both were combined in feedback diagrams without analyses (17, 18). Even though feedback type action was recognized in these diagrams, the servo compensatory implications seem to have been overlooked. Where length-tension effect was represented, analysis was only carried to the point of specifying its effective position in the system. The present study, however, starting from the observation of inertial compensation, lead to the recognition of the need for a feedback effect and from this finally lead back to the recognition of the length-tension curve as that feedback effect.[1] The inclusion of the pulse rate input is an essential consideration if the signal-handling characteristics of the loaded muscle are to be explained.

When this view of muscle is considered, several factors in motor control take on a new meaning. The muscle becomes a controlled positioning device rather than a controlled force motor. The force generated by a particular nerve signal is, in effect, an error signal in a position feedback system and could be quite variable. The stretch reflex can no longer be considered the most peripheral compensating feedback. The muscle feedback in fact provides the compensatory factor to explain why motor control is not totally disrupted by the section of dorsal roots. Muscle feedback can account for, and might have been suspected from, Brown's (3) observations that muscle alone showed a response quite like the stretch reflex when subjected to externally applied stretch. Both the reflex and the muscle, as position control systems with negative position and velocity feedback, would have responses as described in his equations. When supplemented by the muscle feedback loop, the stretch reflex should become a much tighter control system and its residual error should be smaller than can be accounted for by the reflex component alone. If inertial lag is largely compensated by intramuscular feedback it is no longer

[1] See acknowledgments at end of text.

a problem to account for the relatively stable performance of the stretch reflex, even though it contains inertial lag elements, muscle lag elements, and only a limited known lead-producing compensatory capability.

Since much of the length-tension relationship and perhaps the force-velocity effect are now presumed to be the results of the contractile mechanism itself (7), it would appear that the factors which cause this position control feedback–type action are an intrinsic part of the muscle contractile machinery. The previously observed load-compensated response thus seems to be the product of this "position feedback effect" in the sliding filament system. It appears that we may be approaching an explanation of the signal-handling characteristics of loaded muscle in terms of the chemical kinetics of the contraction process itself.

The author wishes to acknowledge the contribution of Miss Amelia Duquette whose dissatisfaction with other attempted explanations of inertial compensation drove him to this analysis and to the supporting experiments. Both she and Mrs. Bonnie Fitzpatrick contributed valuable technical assistance to the conduct of the experiments and manuscript preparation while E. W. Allen made helpful criticisms of the manuscript.

This work was supported by a grant from the Easter Seal Research Foundation.

Received for publication 30 March 1967.

REFERENCES

1. ABBOTT, B. C., and D. R. WILKIE. 1953. *J. Physiol.* (*London*) **120**:214.
2. AUBERT, X. 1956. *Arch. Int. Physiol. Biochim.* **64**:121.
3. BROWN, A. C. 1959. Analysis of the Myotatic Reflex. Ph.D. Thesis. University of Washington. University of Michigan Microfilms, Ann Arbor, Mich.
4. DUCHENNE, G. B. 1949. *Physiology of Motion.* Translated by E. B. Kaplan. J. B. Lippincott Co., Philadelphia, Pa.
5. FENN, W. O. 1938. *J. Appl. Phys.* **9**:165.
6. FENN, W. O., and B. S. MARSH. 1935. *J. Physiol.* (*London*) **85**:277.
7. GORDON, A. M., A. F. HUXLEY, and F. J. JULIAN. 1964. *J. Physiol.* (*London*) **171**:28.
8. HILL, A. V. 1938. *Proc. Roy. Soc.* (*London*) *Ser. B.* **126**:136.
9. HOUK, J. C., JR. 1963. North East Research and Engineering Meeting Record. 138.
10. JEWELL, B. R., and D. R. WILKIE. 1958. *J. Physiol.* (*London*) **143**:515.
11. LEKSELL, L. 1945. *Acta Physiol. Scand. Suppl.* **10**:31.
12. MERTON, P. A., 1953. *Ciba Found. Symp., Spinal Cord.* 247.
13. PARTRIDGE, L. D. 1961. Digest of the 1961 International Conference on Medical Electronics. 105.
14. PARTRIDGE, L. D. 1965. *J. Appl. Physiol.* **20**:150.
15. PARTRIDGE, L. D. 1966. *Am. J. Physiol.* **210**:1178.
16. PRINGLE, J. W. S. 1954. *J. Physiol.* (*London*) **124**:269.
17. PRINGLE, J. W. S. 1960. *Symp. Soc. Exptl. Biol.* **14**:41.
18. ROBERTS, T. D. M. 1966. *In* Nobel Symposium. I. R. Granit, editor. Almqvist & Wiksells, Publishers, Stockholm, Sweden. 457–459.
19. SAVANT, C. J., JR. 1958. Basic Feedback Control System Design, McGraw-Hill Book Company, New York.
20. WAGNER, R. 1927. *Z. Biol.* **86**:397.